CHARA Technical Report

No. 99 08 Apr 2020

CLASSIC J-Band Calibration

G. H. Schaefer, T. A. ten Brummelaar, C. D. Farrington, J. Sturmann, M. Anderson, O. Majoinen, N. Vargas

ABSTRACT: We obtained CLASSIC observations on HD 185395 and HD 210702 on UT 2019 Aug 2−5 in the JHK-band filters. We combined these results with previous observations of the targets in the archive to check the J-band calibration and compare with results obtained at other wavelengths. All of the new and archival data were reduced using the redfluor reduction pipeline. Overall, the J-band data were difficult to collect because the fringes had a low signal-to-noise ratio. The results indicate that the J-band data obtained with CLASSIC calibrates reasonably well, but the magnitude limit is lower ($J < 6$ mag) compared with the H and K-bands.

1. INTRODUCTION

CLASSIC observations in the J-band ($\lambda = 1.286$ μm) extend the spatial resolution of the CHARA Array to 0.38 mas, compared with 0.52 mas in the H-band. Ordinarily, the metrology laser contaminates the signal from the star in the J-band. Notch filters that block the wavelength of the metrology laser were installed on the CLASSIC table in 2013, however, only two J-band brackets on one star have been published thus far (von Braun et al. 2014). We collected additional data in the J-band to test the calibration.

We selected two targets (HD 185395 and HD 201702) that have previous diameters measured with different beam combiners including CLASSIC, MIRC, PAVO, and VEGA over a range of wavelengths. In addition to collecting J-band data, we also collected additional CLASSIC data in the H and K-bands to investigate the cross-filter calibration and cross-combiner calibration.

Recent publications have highlighted discrepancies between the expected and measured diameters in the K-band (Casagrande et al. 2014; White et al. 2018). These discrepancies could be caused by intrinsic calibration errors, errors associated with measuring stellar diameters close to the resolution limit, incorrect models of limb-darkenening and stellar sizes in the K-band, or physical differences in the expected size related to excess circumstellar emission at longer wavelengths. Investigating whether these wavelength dependent size discrepancies persist with more data and understanding the underlying cause is of critical importance, especially as interferometric angular diameters continue to have a more significant impact on the field. For example, Mann et al. (2015) used a sample of 29 stars with interferometric radii measurements to refine methods for determining the effective temper-

[1]Center for High Angular Resolution Astronomy, Georgia State University, Atlanta GA 30303-3083
Tel: (404) 651-2932, FAX: (404) 651-1389, Anonymous ftp: chara.gsu.edu, WWW: http://chara.gsu.edu

atures of K and M dwarf stars. The additional measurements collected for this report help provide a more extensive set of observations collected across different wavelengths bands that could be used to investigate the reliability of interferometric diameters.

Table 1: Observing Log for CLASSIC/MIRC Observations[a]

Target	UT Date	Baseline	Filter	N	Calibrators (HD)	Comment
HD 185395	2007-05-26	S1-E2	*K*	3	183534	Bad calibrator[b]?
	2007-07-19	S1-E1	*K*	11	191195	
	2007-11-02	E2-W1	*K*	5	191195	
	2008-07-25	S1-E1	*K*	8	191195	
	2012-06-19	6T	*H*	1	202850	MIRC
	2019-08-02	S1-E1	*J*	2	177003, 185872	This work
	2019-08-03	S1-E1	*K*	3	177003, 185872	This work
					191195	
	2019-08-04	S1-E2	*J*	2	185872, 191195	This work
	2019-08-05	S1-E2	*J*	3	185872, 191195	This work
HD 210702	2008-09-08	S1-E1	*K*	10	210074	Only 4 published
	2013-08-18	S1-E1	*H*	5	206043, 210074	
	2013-08-18	S1-E1	*J*	2	206043, 210074	
	2013-08-19	E1-W1	*H*	2	206043	Bad shutters in 002
	2013-08-22	E1-W1	*H*	7	210074, 207223	
	2013-08-22	S1-E1	*J*	1	210074, 207223	
	2019-08-03	S1-E2	*J*	2	209166, 210074	This work
	2019-08-04	S1-E2	*J*	5	209166, 210074	This work
	2019-08-05	S1-E2	*J*	2	209166, 210074	This work
	2019-08-05	S1-E1	*K*	3	209166, 210074	This work

[a] All data were collected with CLASSIC except on 2012-06-19 which were taken with MIRC.
[b] HD 183534 looked like a separate fringe packet binary on UT 2019-08-02.

Table 2: Adopted calibrator angular diameters

Cal	LDD	UDD_J	UDD_H	UDD_K	Reference
HD 177003	0.1479 ± 0.0052	0.1461	0.1465	0.1467	JMMC
HD 185872	0.2540 ± 0.0071	0.2498	0.2508	0.2513	JMMC
HD 191195	0.4352 ± 0.0391	0.4263	0.4263	0.4277	JMMC
HD 209166	0.4351 ± 0.0385	0.4263	0.4264	0.4277	JMMC
HD 202850	0.527 ± 0.016				Maestro et al. 2013
HD 206043	0.4012 ± 0.0104	0.3936	0.3936	0.3947	JMMC
HD 210074	0.4115 ± 0.0115	0.4034	0.4034	0.4046	JMMC
HD 207223	0.3477 ± 0.0082	0.3408	0.3408	0.3418	JMMC

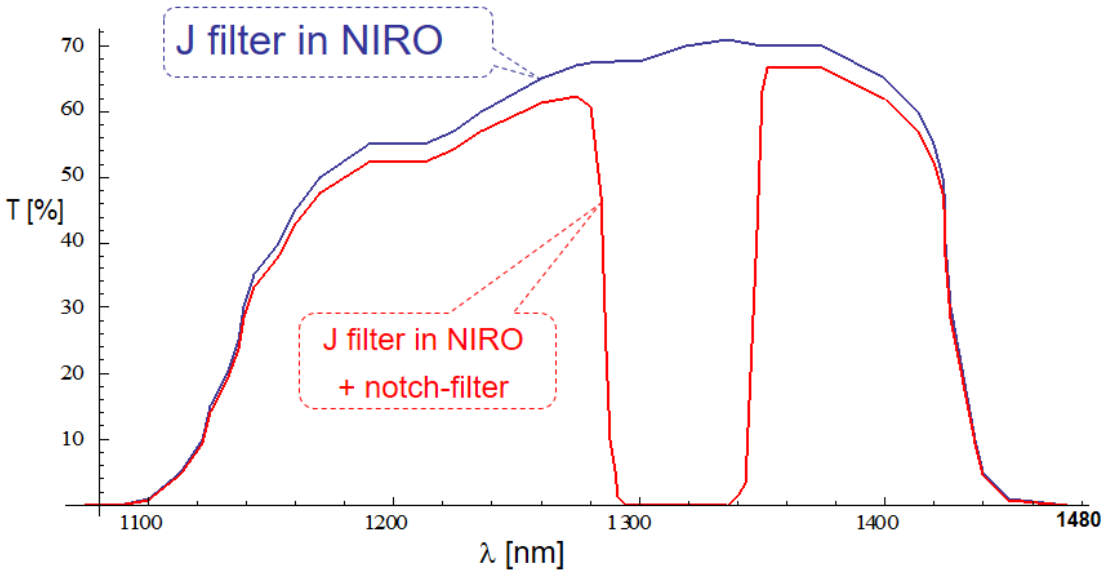

FIGURE 1. J-band filter profile in NIRO with (red) and without (blue) the notch-filter in place. The notch filter causes about a 26% loss of the total J band flux.

2. OBSERVATIONS AND DATA REDUCTION

We collected new CLASSIC observations on HD 185395 and HD 210702 on UT 2019 Aug 2−5. Table 1 lists a log of the observations for all of the new and previously published CLASSIC data on these targets. The table provides the target name, UT date of observation, baseline, filter, number of brackets obtained, and calibrators used. All of the data were reduced using the `redfluor` reduction pipeline, adopting the `V2_MEAN_PS` visibility estimator. For the data recorded in 2007, we converted the old .dat data files into fits format using the routine `irdat2fits`. We calibrated the data using `calibir_linfit` and adopted the uniform disk diameters computed by JMMC (Bourges et al. 2017). The calibrator diameters are listed in Table 2.

Figure 1 shows the profile of the J-band filter in CLASSIC with and without the notch filter in place. The J-band profile is not included in the reduction pipeline, it simply has a top hat function like the rest of the filters with a central wavelength and a width. As long as the calibrator and object are not significantly different in color, we suspect that this should not have a significant impact. It would of course be better to include the true shape of all of the filters convolved with the color temperature of the stars.

We also reduced one night of 6T MIRC data obtained on HD 185395 in the H-band from UT 2012-06-19 that was previously published by White et al. (2013). We reduced and calibrated the data using the IDL MIRC pipeline written by John Monnier. The calibrator HD 202850 was observed before and after HD 185395, however, there was a large jump in the raw visibility between the two calibrator observations. We discarded the first calibrator observation because it was observed at low elevation ($< 40°$) and the visibility was lower than that of the target. It was also the first observation of the night and could have been impacted by dome seeing. The second observation of the calibrator was taken at a similar elevation as the target ($\sim 65°$). HD 202850 is a well used calibrator for MIRC.

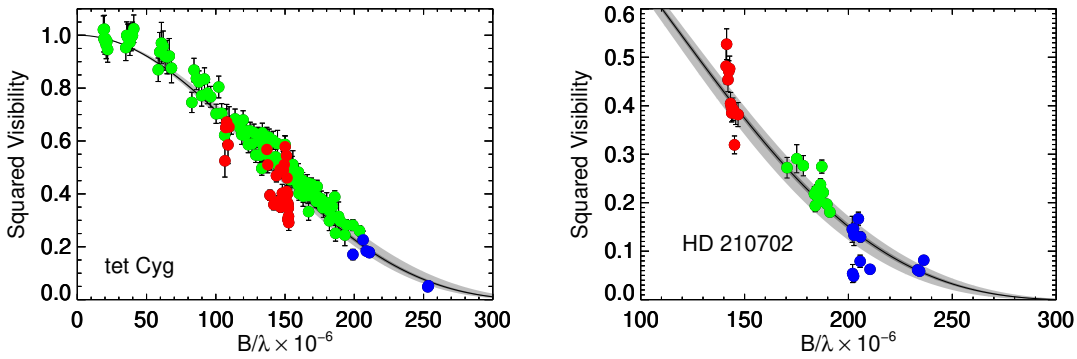

FIGURE 2. *Left:* Classic JK and MIRC H-band visibilities measured for HD 185395 (θ Cyg). *Right:* Classic JHK visibilities measured for HD 210702 (HR 8461). In both panels, the measured values are color-coded by wavelength (J is blue, H is green, and K is red).

3. ANGULAR DIAMETERS

We computed uniform disk ($\theta_{\rm UD}$) and limb-darkened disk ($\theta_{\rm LD}$) diameters separately for each wavelength band by minimizing the χ^2 between the measured and model visibilities. For the limb-darkened model, we also fit the JHK visibilities simultaneously. The uncertainties were estimated through a bootstrap technique as described in Schaefer et al. (2018). The new results are shown in the bottom portion of Table 3. For comparison, the top portion shows the previous results reported in the literature. For the limb-darkening coefficients (μ_λ), we adopted the same values that were used in the literature, as summarized in Table 3. The middle portion of the table gives the uniform and limb-darkened disk diameters computed by JMMC (Bourges et al. 2017). The measured visibilities and limb-darkened fits are shown in Figure 2.

Figure 3 shows a comparison of the limb-darkened angular diameters for HD 185395 and HD 210702. Each panel shows the new diameters measured in each wavelength band, as well the combined fit based on all of the JHK data. We also plot the previously measured diameters reported in the literature. For HD 185395, there is good consistency between the R-band limb-darkened diameter measured with PAVO and VEGA, the combined JHK fit, and the JMMC estimate. However, there is a larger discrepancy between the individual fits the to J, H, and K-bands. For HD 210702, all of the JHK fits are fairly consistent with each other, however, the infrared results produce larger diameters compared with the R-band PAVO measurement and the expected diameter computed by JMMC.

4. SENSITIVITY TESTS

On UT 2019-08-02, we attempted to record J-band fringes on progressively fainter targets. We succeeded in recording weak fringes on HD 219487 ($J = 5.8$ mag) as shown in Figure 4. However, the fringes were barely detectable on HD 219538 ($J = 6.5$ mag) as shown in Figure 5. Therefore, we estimate that the sensitivity limit in good conditions is $J < 6$ mag.

Table 3: Angular diameters measured for HD 185395 (θ Cyg).
[V=4.48, J=4.76, H=3.72, K=3.52]

Combiner	Filter	N(V^2)	$\theta_{\rm UD}$ (mas)	μ_λ	$\theta_{\rm LD}$ (mas)	Reference
VEGA	R	25	0.726 ± 0.007	0.355	0.749 ± 0.008	Ligi et al. 2016
PAVO	R	19	0.720 ± 0.004	0.47	0.754 ± 0.004	White et al. 2013
MIRC	H	120	0.726 ± 0.014	0.21	0.739 ± 0.014	White et al. 2013
CLASSIC	K'	25	0.845 ± 0.015	0.200	0.861 ± 0.015	Boyajian et al. 2012
JMMC					0.751 ± 0.070	Bourges et al. 2017
JMMC	R		0.718			Bourges et al. 2017
JMMC	J		0.736			Bourges et al. 2017
JMMC	H		0.736			Bourges et al. 2017
JMMC	K		0.738			Bourges et al. 2017
MIRC	H	120	0.713 ± 0.004	0.21	0.724 ± 0.004	This work
CLASSIC	J	7	0.775 ± 0.007	0.21	0.790 ± 0.007	This work
CLASSIC	K'	27	0.811 ± 0.018	0.20	0.824 ± 0.018	This work
ALL	JHK	154			0.761 ± 0.008	This work

Table 4: Angular diameters measured for HD 210702 (HR 8461).
[V=5.93, J=4.51, H=4.00, K=3.98]

Combiner	Filter	N(V^2)	$\theta_{\rm UD}$ (mas)	μ_λ	$\theta_{\rm LD}$ (mas)	Reference
PAVO	R	9	0.778 ± 0.007	0.63	0.831 ± 0.011	White et al. 2018
CLASSIC	JH	2J, 14H	0.845 ± 0.005	0.484	0.886 ± 0.006	von Braun et al. 2014
CLASSIC	K'	4	0.854 ± 0.017	0.31	0.875 ± 0.018	Baines et al. 2009
JMMC					0.779 ± 0.083	Bourges et al. 2017
JMMC	R		0.735			Bourges et al. 2017
JMMC	J		0.759			Bourges et al. 2017
JMMC	H		0.759			Bourges et al. 2017
JMMC	K		0.762			Bourges et al. 2017
CLASSIC	J	12	0.840 ± 0.017	0.484	0.881 ± 0.017	This work
CLASSIC	H	13	0.816 ± 0.006	0.484	0.853 ± 0.007	This work
CLASSIC	K'	13	0.835 ± 0.012	0.484	0.871 ± 0.014	This work
ALL	JHK	38			0.868 ± 0.007	This work

5. SUMMARY

In this Technical Report, we show that visibilities measured in the J-band with CLASSIC provide consistent results when compared with measurements in the H and K-bands. Systematic offsets between measurements in the same filter and across different filters are sometimes present, so it is important to collect a sufficient number of observations to minimize the impact of systematic errors. Ellyn Baines conducted a comprehensive analysis based on a large number of visibility measurements at NPOI to determine that on the order of $\sim 25{-}30$ independent visibility measurements are needed for a reliable diameter measurement (personal communication, 2020).

Observing in J-band with CLASSIC is slow and challenging because of the low signal-to-noise fringes. The H and K-band data on HD 185395 and HD 210702 were typically

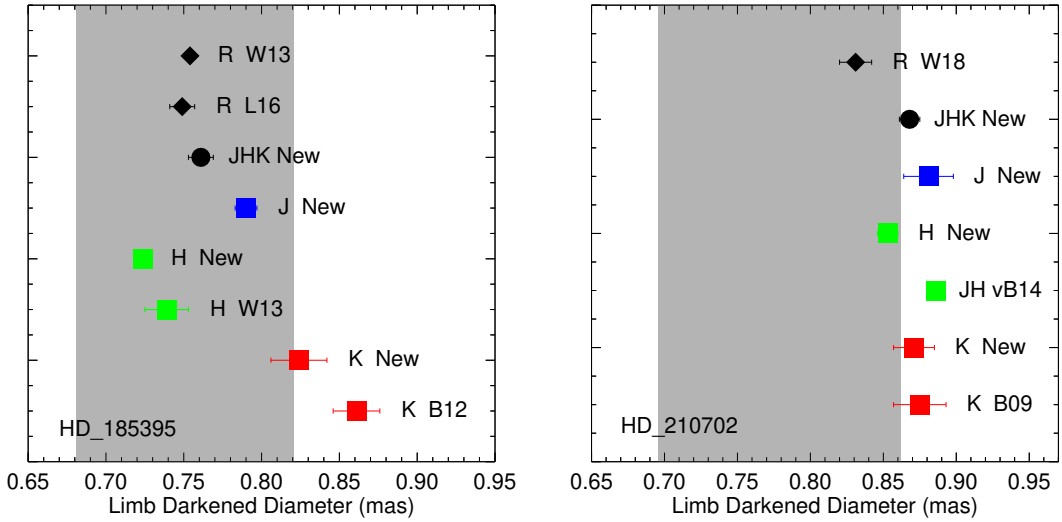

FIGURE 3. Comparison of limb-darkened angular diameters measured for HD 185395 (left) and HD 210702 (right). The shaded gray region represents the limb-darkened angular diameter and error computed by JMMC (Bourges et al. 2017). Each diameter measured interferometrically is labeled with the wavelength filter used and the reference (New = this work; B09 = Baines et al. 2009; B12 = Boyajian et al. 2012; W13 = White et al. 2013; vB14 = von Braun et al. 2014; L16 = Ligi et al. 2016; W18 = White et al. 2018).

recorded at 750−1000 Hz with few scans flagged as having low SNR. In comparison, we needed to record the J-band data at 500−750 Hz; the number of low SNR scans typically exceeded the number of good data scans. To finish the J-band brackets in a reasonable amount of time, we ended up clicking the "SKIP LOW SNR" button on Cosmic Debris and recording $\sim$ 300 scans regardless of data quality. Alternatively, one could adjust the SNR threshold to a lower value in the CLASSIC GUI.

Despite the difficulties with collecting J-band data, the results presented here indicate that it can be used as a valid method to extend the angular resolution of the CHARA Array in the near-infrared with a sensitivity limit of $J < 6$ mag. If one considers observing in the J-band, we suggest collecting data at multiple wavelengths (JHK) as a check on the calibration.

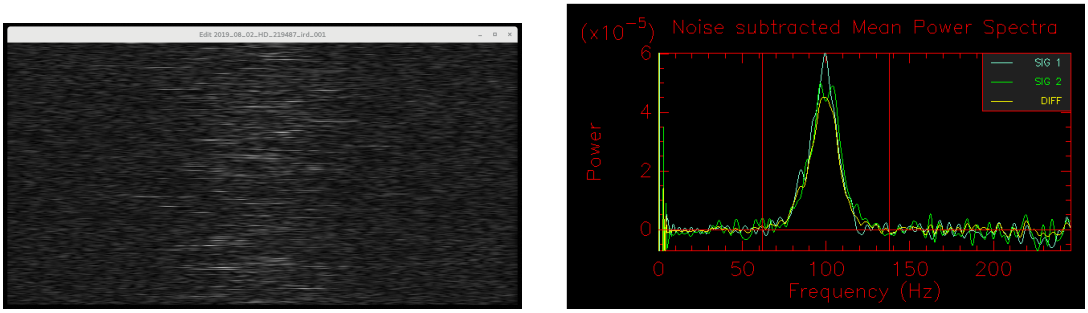

FIGURE 4. Fringe waterfall (left) and mean power spectrum (right) measured for HD 219487 ($J = 5.8$ mag) using CLASSIC in the J-band on UT 2019-08-02.

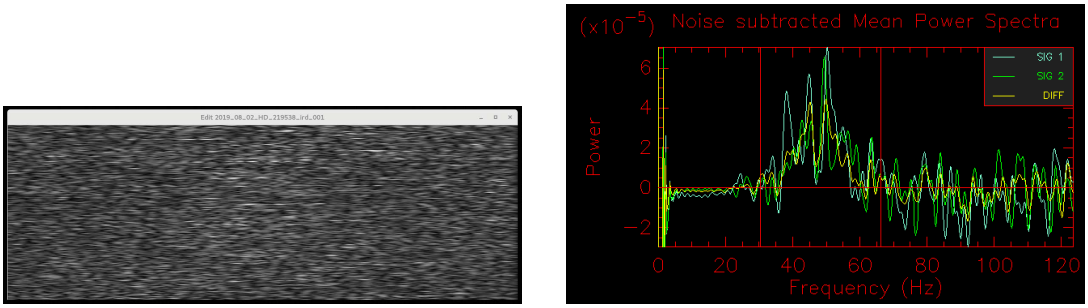

FIGURE 5. Fringe waterfall (left) and mean power spectrum (right) measured for HD 219538 ($J = 6.5$ mag) using CLASSIC in the J-band on UT 2019-08-02.

6. REFERENCES

Baines, E. K., McAlister, H. A., ten Brummelaar, T. A., et al. 2009, *ApJ*, 701, 154
Bourgés, L., Lafrasse, S., Mella, G., et al. 2014, *Proc: ASPC conference on Astronomical Data Analysis Software and Systems XXIII*, 485, 223
Boyajian, T. S., McAlister, H. A., van Belle, G., et al. 2012, *ApJ*, 746, 101
Casagrande, L., Schönrich, R., Asplund, M., et al. 2011, *A&A*, 530, A138
Ligi, R., Creevey, O., Mourard, D., et al. 2016, *A&A*, 586, 94
Mann, A. W., Feiden, G. A., Gaidos, E., et al. 2015, *ApJ*, 804, 64
Maestro, V., Che, X., Huber, D., et al. 2013, *MNRAS*, 434, 1321
Schaefer, G. H., White, R. J., Baines, E. K, et al. 2018, *ApJ*, 858, 71
von Braun, K., Boyajian, T. S., van Belle, G. T., et al. 2014, *MNRAS*, 438, 2413
White, T. R., Huber, D., Maestro, V., et al. 2013, *MNRAS*, 433, 1262
White, T. R., Huber, D., Mann, A. W., et al. 2018, *MNRAS*, 477, 4403